INVESTIGATION OF THE FAILURE MECHANISMS FOR DELAMINATION GROWTH FROM EMBEDDED DEFECTS

E. Greenhalgh and S. Singh

Mechanical Sciences Sector, DERA, Farnborough, GU14 0LX, UK

SUMMARY: Delamination growth from single-plane embedded defects has been investigated in laminated composite plates under compressive loading. The damage mechanisms were only weakly affected by the size and shape of an implanted defect, but very significantly affected by its location through the stacking sequence. In general, delamination growth did not occur at a single plane but rather on several planes. The most critical ply interfaces for delamination growth were those where the ply nearer the free surface had fibres oriented transverse to the principal compressive loading direction. The results are relevant for assessing the severity of damage in-service and in damage-tolerant structural design.

KEYWORDS: delamination, failure mechanisms, compression, embedded defects, stacking sequence, fractography, Moiré interferometry.

INTRODUCTION

Models for predicting the strength of composite structures under general loading conditions are not sufficiently accurate, due to the poor understanding of damage and its effects upon failure. Development and certification rely on expensive testing and rarely result in the optimum exploitation of materials; thus the potential benefits of using composites are not being realised. Tolerance to delamination is a key design requirement since this can significantly degrade compressive performance [1]. The best models, while adequate for predicting delamination initiation, do not predict the later damage mechanics that ultimately determine component strength. These mechanisms need to be studied and modelled [2].

The aim of this work was to understand how the characteristics of a defect affect the mechanisms of delamination growth. The defects were single-plane artificial delaminations, the sizes, shapes and positions of which were comparable to damage observed in studies on low-velocity impact of structural elements [1,3]. The approach was to test laminates under controlled conditions, using Moiré interferometry to monitor the damage growth. Fractographic techniques were used to deduce the damage growth mechanisms. Subsequently, rules for damage tolerant design and modelling delaminations were derived.

EXPERIMENTAL DETAILS

Laminates, 3mm thick, were manufactured from Hexcel T800/924 carbon/epoxy with a quasi-isotropic lay-up of $[(+45°/-45°/0°/90°)_3]_S$. A defect consisting of a 10μm thick PTFE film was included, at a depth either of 3 plies (0°/90° interface) or 5 plies (+45°/-45° interface). These relatively shallow depths were chosen to be representative of backface delamination in impact damage. Details of the defect sizes, shapes and locations are shown in Table 1.

	Implanted Defect Details				
Panel	**Size (mm)**	**Shape**	**Depth (Interface)**	**Area**	**Initiation**
A	35	●	3 (0°/90°)	962mm²	2400με
B	50	●	3 (0°/90°)	1964mm²	2400με
C	35 x 50	⬮	3 (0°/90°)	1374mm²	3350με
D	50 x 71	⬮	3 (0°/90°)	2788mm²	1850με
E	35	●	5 (+45°/-45°)	962mm²	4150με
F	50	●	5 (+45°/-45°)	1964mm²	3150με
G	35 x 50	⬮	5 (+45°/-45°)	1374mm²	3150με
H	50 x 71	⬮	5 (+45°/-45°)	2788mm²	2950με
I	50	●	3 (0°/90°)	1964mm²	1950με

Table 1: Defect details and delamination initiation strains

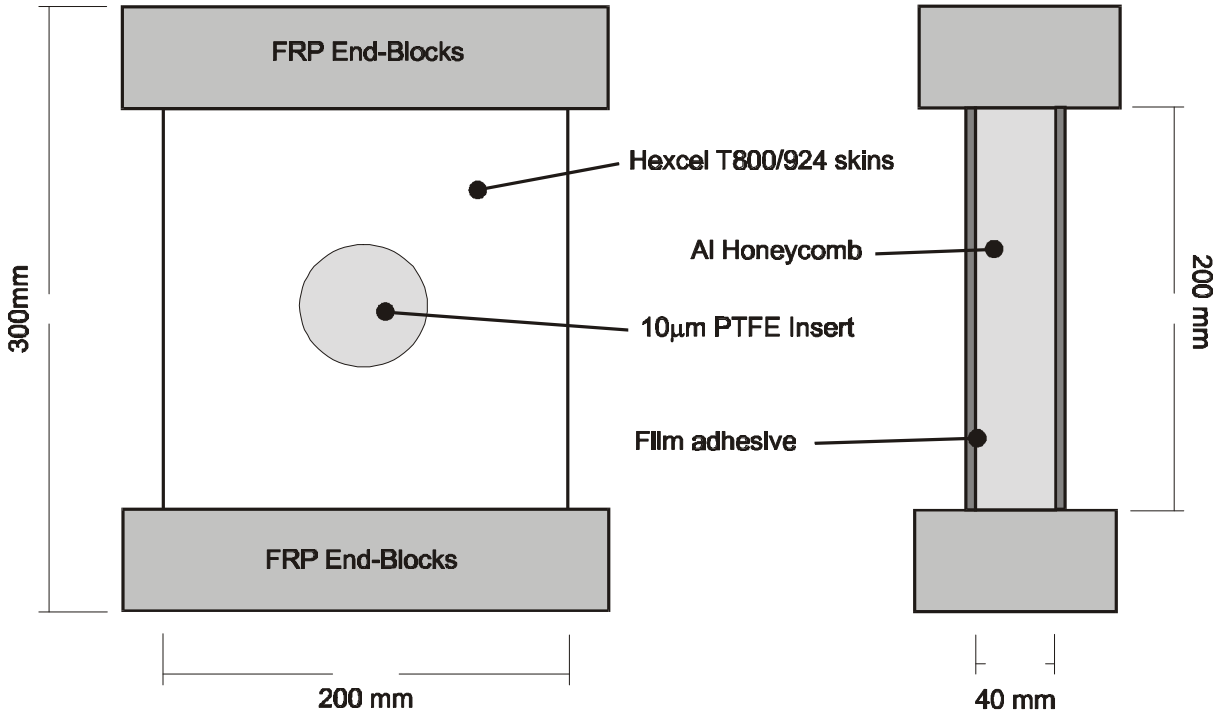

Figure 1: Geometry and strain gauge positions for the honeycomb panels

The laminates were supported using an aluminium honeycomb core (Figure 1) to form sandwich panels. These panels were stabilised against buckling to strains up to -10000με, eliminating the need for an anti-buckling guide and the associated complications [4]. The damage growth was monitored using shadow Moiré interferometry which was calibrated using

a wedge [4]. The panels were loaded in compression at a rate of 0.3mm/min until the damage had approached the panel edges. After testing, the panels were ultrasonically scanned to determine the damage extent, and the fracture surfaces were dissected and and examined using electron microscopy. With reference to fracture surfaces generated under controlled conditions, the loading conditions during failure were deduced. In particular, the proportion of mode I and II fracture at different sites were determined from the tilt of the cusps [5].

EXPERIMENTAL RESULTS AND FAILURE ANALYSES

Panels Containing Defects Three Plies Deep (0°/90° Ply Interface)

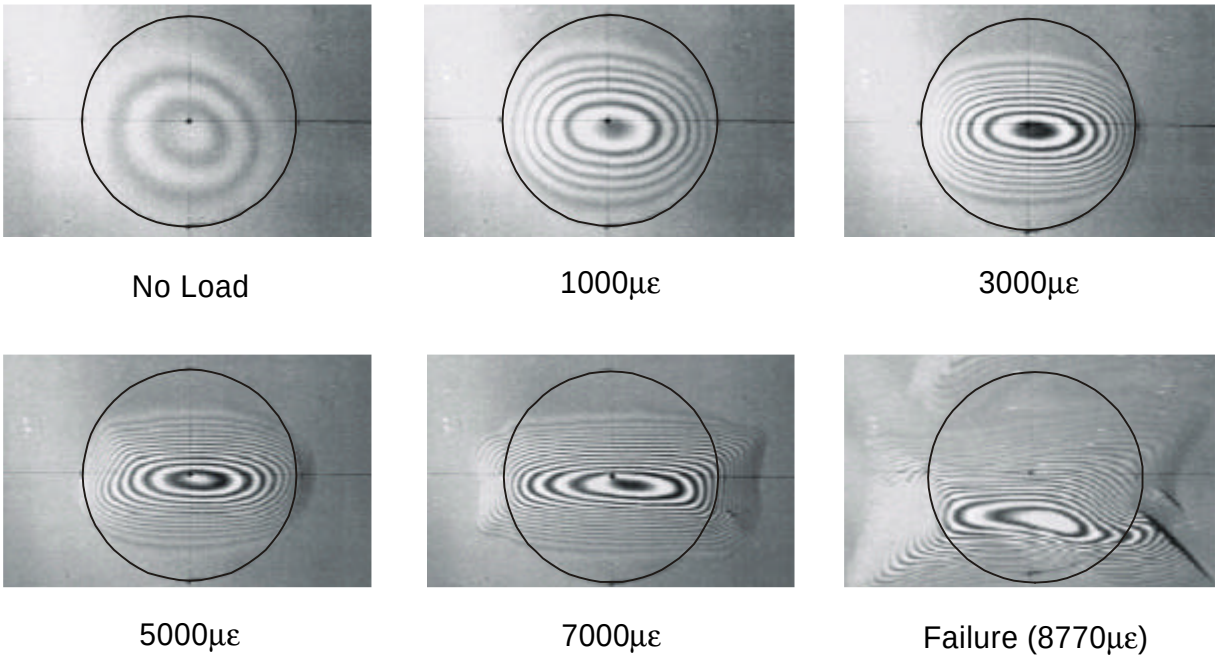

Figure 2: Damage growth from 50mm defect three plies deep (0º/90º ply interface)

The typical damage evolution from defects three plies deep is shown in Figure 2. As the load was introduced, the delaminated region became elliptical, with the peak deflection increasing, until growth initiated at the transverse boundaries of the defect. Initiation occurred at applied strains of between -1850με and -3350με (although there was a large uncertainty associated with these values). The delamination formed a lozenge shape, with lobes growing on the right side, from just above the major axis of the ellipse and, on the left side, from just below the major axis, nearly parallel to the -45° ply. Secondary growth initiated from the transverse boundary of the damage and propagated parallel to the +45° ply. At a higher applied strain (-6000με), the delamination developed into a rectangle and finally into a dog-bone shape. Rapid growth of the corner lobes occurred, followed by splitting of the surface plies. Finally, there was longitudinal damage growth from the axial boundary of the insert.

For all the defects three plies deep the out-of-plane deflections increased linearly with applied strain until near failure, when the deflections increased at a faster rate (Figure 3). For a given applied strain the deflections of panels A and C (35mm insert width) were approximately 0.5mm lower than those in panels B, D and I (50mm insert width). After initiation, the

delamination width steadily increased, becoming unstable at the end of the test (Figure 4). Comparison between results from panels B and I indicated little specimen variability.

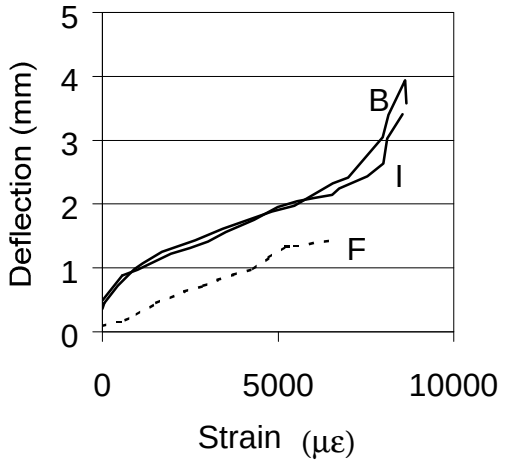

Figure 3: Out-of-plane deflections for 50mm circular defects three and five plies deep

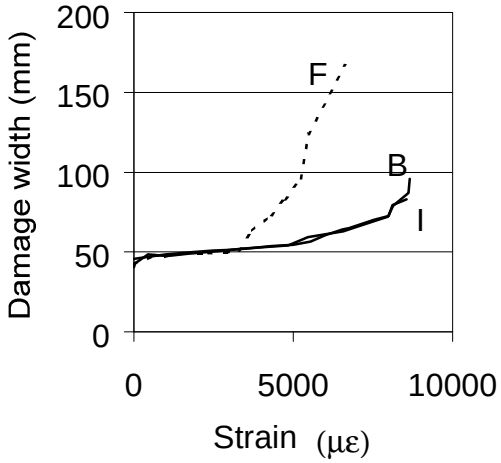

Figure 4: Damage widths for 50mm circular defects three and five plies deep

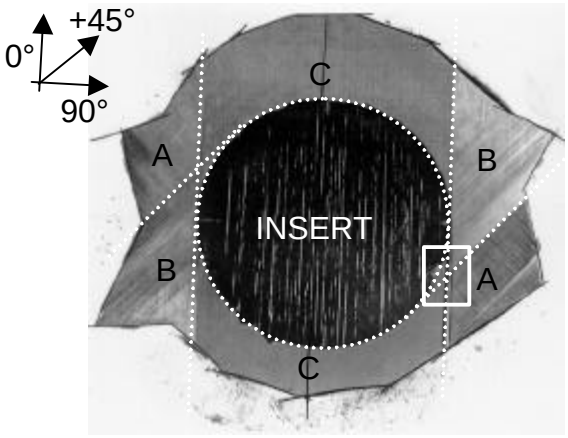

Figure 5: Damage growth from defect three plies deep (0°/90° interface) (lower surface)

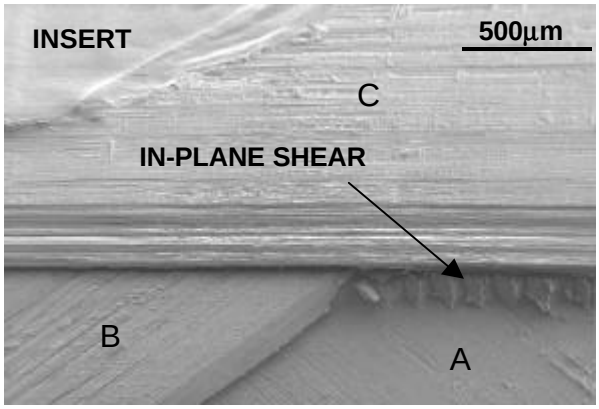

Figure 6: Micrograph of delaminated plies from surface matching Figure 5.

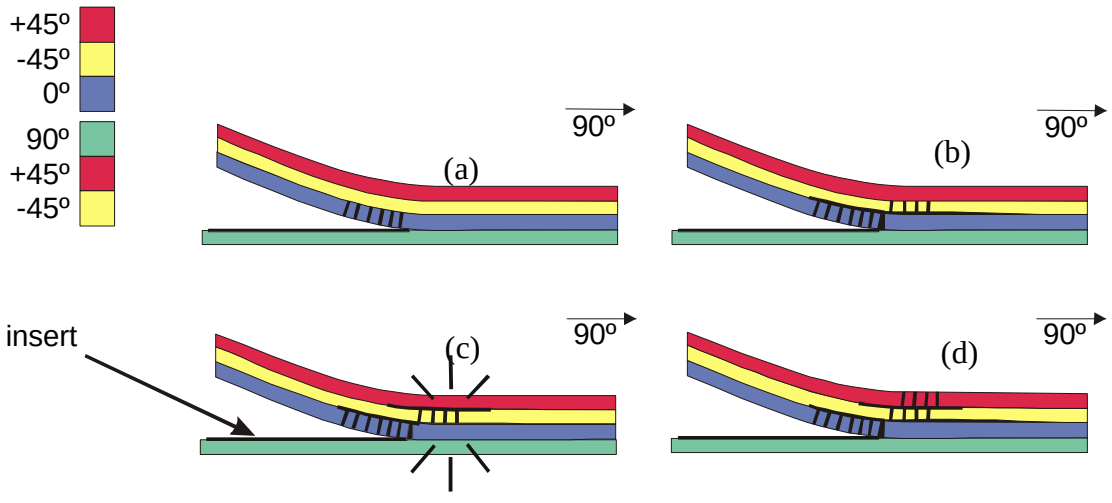

Figure 7: Damage sequence from defects 3 plies deep (0°/90° ply interface)

The damage surfaces from a 50mm circular defect located at the 0°/90° ply interface (panel I) are shown in Figure 5. The fracture surfaces and mixed-mode distributions exhibited rotational symmetry. Figure 6 is a micrograph of part of the delaminated material matching the surface from the substrate in Figure 5 and illustrates the different damage planes and failure modes.

Figure 7 shows the growth processes in the panels with defects at the 0°/90° ply interfaces. Firstly (Figure 7a), the tensile Poisson strains and curvature across the ply directly above the defect plane (0°) had led to the development of splits, tangential to the defect boundary. The delamination migrated through these splits (Figure 7b) and extended into the 2/3 (-45°/0°) ply interface (zone B in Figure 5). Within this interface the delamination had then grown parallel to the –45° ply as a mixed-mode fracture. Splits had also developed in the –45° ply (Figure 7b), through which the delamination migrated into the 1/2 (+45°/-45°) ply interface (zone A in Figure 5). The delamination had then grown within this interface, parallel to the +45° ply (Figure 7c) again as a mixed-mode fracture. The combined extension of these two zones gave rise to the elliptical, rectangular and finally dog-bone shaped damage contours. Ultimately, splits developed in the surface ply (Figure 7d) which alleviated the local driving forces at the crack tip and arrested the damage growth. Late in the growth process, the in-plane shear forces were high enough to cause fibre fracture (Figure 6). Finally, mode II delamination growth had occurred at the defect plane (zone C in Figure 8), at the axial extents of the insert.

Panels Containing Defects Five Plies Deep (+45°/-45° Ply Interface)

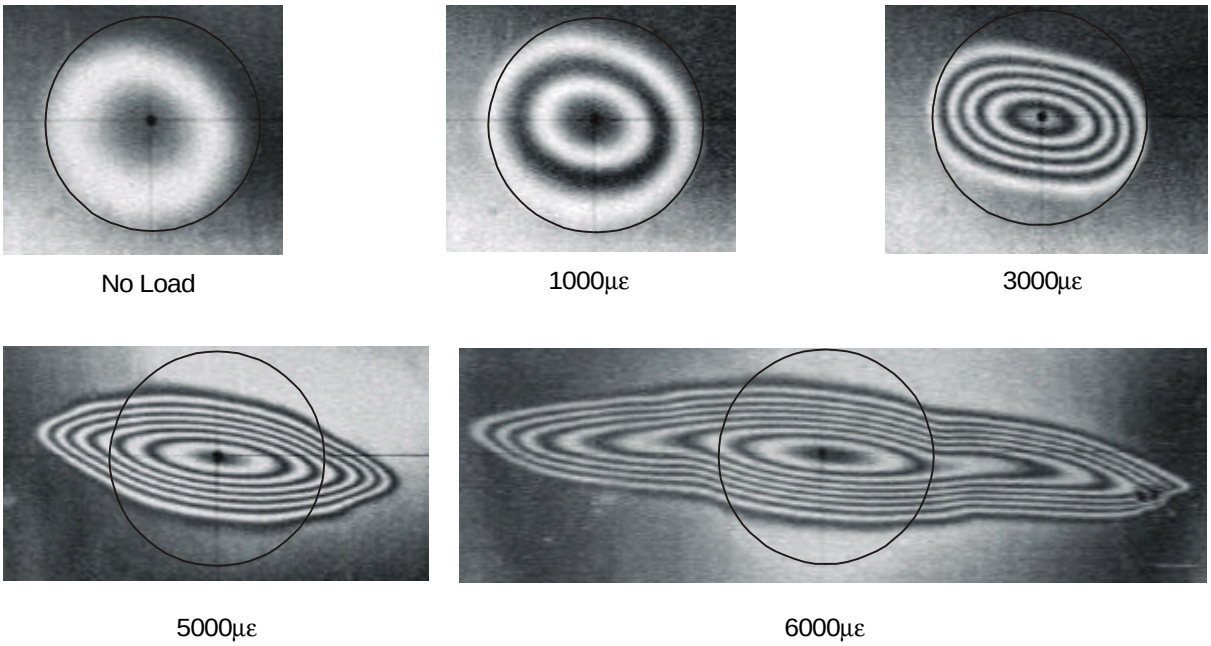

Figure 8: Damage growth from a 50mm defect five plies deep (+45º/-45º ply interface)

The damage evolution from defects five plies deep differed from that from defects three plies deep, as shown in the Moiré images in Figure 8. As the load was applied, the delaminated region became elliptical, with the major axis at about 105° (clockwise) to the loading direction. At an applied strain of between -2950με and -4150με, delamination growth initiated at opposing points on the defect boundary at about 100° to the loading direction. The delamination extended from these points (as slip-stick growth), developing into a flattened ellipse until the tests were stopped at applied strains of between -6000με and -6900με.

For all the defects five plies deep, the out-of-plane deflections were linear for the entire test (Figure 3) but the deflections were almost 1mm lower than for the defects three plies deep.

After initiation, the damage width increased almost linearly for most of the test (Figure 4). For a given applied strain, the damage in panels F and H (50mm insert) had extended about 20mm further than the damage in panels E and G (35mm insert). Perhaps unexpectedly, the damage grew much faster from the defects five plies deep than from those three plies deep.

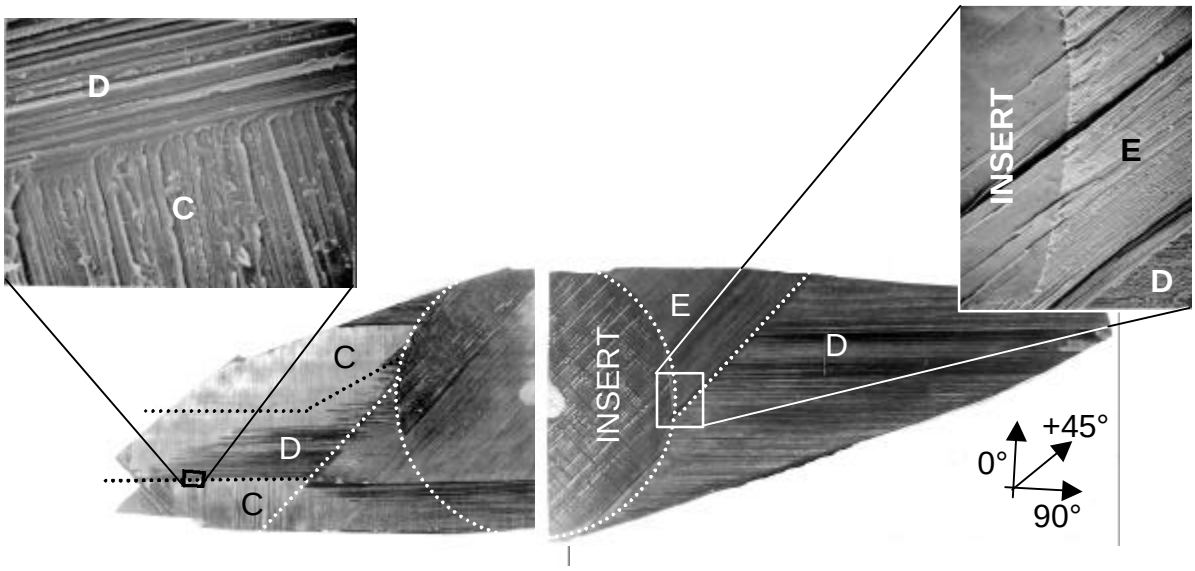

Figure 9: Damage growth from defect five plies deep (+45º/-45º interface) (upper surface)

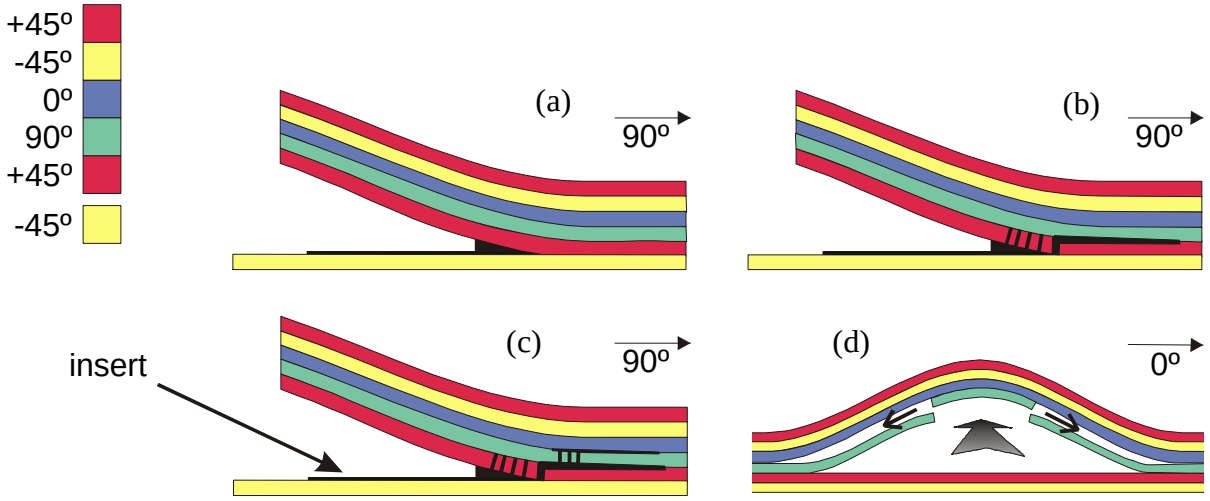

Figure 10: Damage sequence from defects five plies deep (+45°/-45° ply interface)

Figure 9 shows a typical damage surface (panel E) from a defect five plies deep (+45º/-45º ply interface) whilst Figure 10 illustrates the damage growth processes in these panels. Unlike the panels with defects at the 0°/90° ply interface, the delamination failure initiated at the defect plane (Figure 10a) and extended as a mixed-mode fracture parallel the +45° ply (zone E in Figure 9). Splits then developed in this ply, through which the delamination migrated before extending along the 90° plies in the adjacent +45°/90° interface (Figure 10b). The delamination continued to grow quite rapidly within this interface (zone D in Figure 9), as a mode I dominated fracture.

On the left half of Figure 9, the fourth (90º) ply had been removed from the specimen during dissection, exposing two delamination zones C, three plies deep (0º/90º ply interface). This fracture surface was mode I dominated near zones D and mode II dominated nearer its outer

boundaries. Splits had developed in the 90° ply (Figure 10c), through which the delamination migrated into this 0°/90° layer, where it grew parallel to the 0° ply (zone C in Figure 9). Zones C and D had been generated simultaneously, as illustrated in Figure 10d.

DISCUSSION

Delamination initiation and growth were controlled by the mode I (peel) and mode II (shear) forces at the defect boundary. The location and magnitude of the maxima of these components were dictated by the buckle shape of the delaminated material, which in turn was controlled by the stacking sequence of the delaminated plies. Although some of the initial defects were circular, the uniaxial compressive load always generated an elliptical blister with the major axis nearly transverse to the loading direction. This elliptical shape can be attributed to the curvatures around the defect boundary. The damage blister resulted in outward (opening) curvature of the delaminated plies all around the defect edge. Parallel to the loading axis, the applied compressive strains superimposed a closing curvature on the delaminated plies, resulting in an increased mode II loading. In contrast, perpendicular to the loading axis, the opening curvatures caused by the tensile Poisson strains enhanced the mode I loading.

The stacking sequence of the delaminated material also contributed to the blister shape. If the stacking sequence of these plies had been balanced, as it nearly was for defects at the 0°/90° ply interface, the minor axis of the ellipse would have been aligned with the loading direction. When the delaminated plies were not balanced, as for defects at the +45°/-45° ply interface, stiffness coupling terms led to rotation of the ellipse and consequently rotation of the positions of the mode I and II maxima.

The depth in which the initial defect was located had a strong influence on the delamination initiation and growth. In general, the delaminations from the defects three plies deep initiated at a lower strains than from defects five plies deep. For a given strain, in the shallower defects the lower bending stiffness led to greater opening curvatures at the insert boundary and lower initiation strains. Initiation from the defect at the 0°/90° ply interface was further promoted by the 0° ply splits which introduced opening forces that initiated new delamination sites; these splits have been shown to have formed at an applied strain of about –1500με [7].

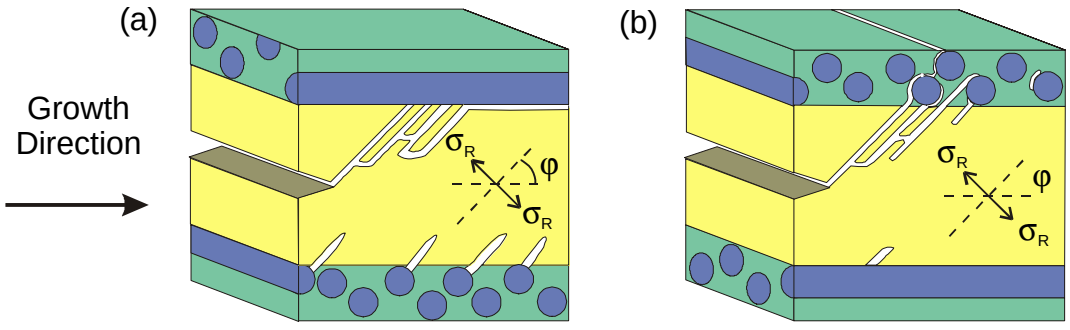

Figure 11: Comparision between crack growth at (a) 0°/ϕ° and (b) ϕ°/0° ply interfaces

The orientations of the delaminated plies were also an important factor in the delamination growth. For these panels, in which global buckling was inhibited, cracks were driven from the insert plane through the delaminated plies towards the outer surface. As illustrated in Figure 11a, when the growth direction and the fibres of the outer (uppermost) ply of the interface were approximately aligned, the delamination remained within that plane and growth was

rapid. When these fibres were oblique to the growth direction (Figure 11b), the cracks were not constrained and migrated upwards into the next interface. Fuller explanations of delamination migration and local growth directions are given elsewhere [6].

As a consequence of the migration effects, the delamination growth was governed by the location of the initial defect. The damage growth from defects three plies deep was slow, whilst defects five plies deep extended rapidly. Mode I forces drove the delamination growth and were greatest approximately transverse to the applied load. For defects three plies deep, there were no fibres above the initial defect which were aligned with this driving force. Since delamination growth is locally parallel to the uppermost fibres of an interface, delamination growth could only occur at 45º to this driving force in zones B and A (Figure 5), reducing the growth rate. The axial component to the growth in these zones also led to an increase in the mode II loading, increasing the resistance to growth [4]. For defects five plies deep, however, the crack was able to migrate from the insert to the zone D (90º/+45º ply interface), where the 90º fibres above the interface were closely aligned with this driving force. Consequently delamination growth was mode I dominated and was rapid.

Although the main controlling factors on the damage growth mechanisms were the initial defect depth and ply interface, the defect size and shape did have a limited influence. Evidence that the larger defects exhibited a lower initiation strain than the smaller defects agreed with the trends in the literature [4]. For the defects five plies deep the initiation strain was inversely proportional to the damage deflection. This indicated that the length of the defect influenced the degree of longitudinal bending of the delaminated material, which in turn controlled the degree of lateral bending of these plies. The greater the lateral bending, the greater the curvature at the transverse boundary of the insert, and hence the lower the initiation strain. A similar effect may have been present for the defects three plies deep.

For both sets of panels, fractographic analysis showed that the damage growth processes and mixed-mode conditions were relatively independent of the initial defect size. There was some evidence for a larger mode II component in the damage associated with the larger defects. This may be attributed to the increase in the strain difference between the delaminated material and the sublaminate for the larger defects, as discussed by Purslow [8].

These results suggest design rules for constraining delamination growth by appropriate selection of the stacking sequence. A delamination at an interface between two plies will tend to grow parallel to the fibres in the ply which is nearest the surface. It can migrate through the plies to interfaces even closer to the surface, but it always grows parallel to the fibre directions. For design, the critical depth for delamination growth under in-service loads should be determined from the predicted mode I component, and then the stacking sequence of the outer material within this critical depth should be engineered to ensure that none of the ply directions are coincident with the driving forces. For example, in skin-stringer panels under compression this would mean there should be no 90º plies in the outer material within the critical depth [9].

Current numerical modelling of delamination growth from embedded defects assumes the damage growth is in the same plane as the initial defect. The work described in this paper has shown that this is very different from reality. In some cases, the first delamination growth is on a different plane to the initial defect (closer to the surface). Although such models may have limited success in predicting delamination initiation, the later stages of damage growth need to be modelled more realistically. A more successful predictive approach would be to include

simple rules, such as preferential growth directions, and mechanisms such as ply cracking and fibre fracture.

CONCLUSIONS

Delamination growth from implanted defects in CFRP panels under compressive loading were investigated. From these studies the following conclusions have been drawn:

1. Delamination initiation and growth were governed by the peel (mode I) and shear (mode II) forces at the defect boundary. The buckle shape of the delaminated material determined the maxima. The mode I maximum, which was the main driving force for delamination growth, was approximately transverse to the applied load.

2. Stiffness coupling at the delaminated plies can act to rotate the damage blister, shifting the positions of the mode I maxima and consequently affecting the growth rate. This stiffness coupling must be represented in models; quarter-model symmetry may not be assumed.

3. The initial defect size and shape had little effect on the damage processes; the depth of the defect and the ply orientations in the delaminated material had most effect. Shallower delaminations initiated at lower loads.

4. Delamination growth from a single plane defect did not occur at one plane but on several planes, with mechanisms such as ply cracking and fibre fracture also occurring. Delamination growth at a ply interface was always parallel to the fibres in the ply nearer the surface; cracks would migrate through plies to interfaces still closer to the surface.

5. In structures such as stringer-stiffened panels, transverse delamination growth will be most detrimental. If there are no 90° plies in the delaminated material then transverse growth will be significantly less and will be diverted along both +45° and -45° plies. If there are 90° plies, then damage will reach the stringers where it may promote stringer detachment from the skin. Delamination growth can also be inhibited by tailoring the geometry to constrain bending and buckling of delaminated material, thus reducing peel.

6. For damage tolerant design the critical depth for delamination growth under in-service loads should be determined from the predicted mode I component, and then the stacking sequence of the outer material within this critical depth should be engineered to ensure that none of the ply directions are coincident with the peak driving forces.

7. Current numerical modelling of delamination growth assumes the damage growth is in the same plane as the initial defect; this work has demonstrated that this is very different from reality. A better approach would be to include simple rules such as preferential growth directions and mechanisms such as transverse cracking and fibre fracture.

8. The understanding of delamination growth processes obtained in this work allows some prediction of the severity of damage which may occur in service in composite structures. It could also be utilised to produce damage tolerance in new structural designs and develop physically based predictive models.

ACKNOWLEDGEMENTS

MoD Package 07B and DTI CARAD are acknowledged for their support. The authors also acknowledge the contributions of the DERA staff and Frank Matthews (Imperial College).

REFERENCES

1. Gadke M., *et al*, 'GARTEUR Damage Mechanics for Composite Materials; Analytical/Experimental Research on Delaminations', In '*Debonding/Delamination of Composites - 74th AGARD Structures & Materials Panel*', Patras, Greece, 1992.

2. Lagace P., 'Delamination: From Initiation to Final Failure', *Proceedings of the Ninth International Conference on Composite Materials*, Madrid, Spain, Ed. A. Miravete, Vol. 1, 1993, pp120-122.

3. Greenhalgh E., Bishop S., Bray D., Hughes D., Lahiff S. and Millson B., 'Characterisation of Impact Damage in Skin-Stringer Composite Structures', *Composites Structures*, Vol 36, 1997.

4. Greenhalgh E., '*Characterisation of Mixed-mode Delamination Growth in Carbon-Fibre Composites*', PhD Thesis, Imperial College, London, 1998.

5. Greenhalgh E. and Matthews M., 'Characterisation of Mixed-Mode Fracture in Unidirectional Laminates', *Proceedings of the Seventh European Conference on Composite Materials*, London, 1996.

6. Singh S. and Greenhalgh E., 'Micromechanisms of Interlaminar Fracture in Carbon-Fibre Reinforced Plastics at Multidirectional Ply Interfaces Under Static and Cyclic Loading', *Plastics, Rubber and Composites Processing and Applications*, Vol 27, 1998.

7. Lord S. and Greenhalgh E., 'Analysis and Prediction of Delamination Growth from Embedded Defects in Composite Materials', *Proceedings of the Eighth European Conference on Composite Materials*, Naples, 1998.

8. Purslow D., 'Matrix Fractography of Fibre Epoxy Composites', RAE Technical Report 86046, 1986.

9. Greenhalgh E., Singh S. and Nilsson K-F, 'Mechanism and Modelling of Delamination Growth and Failure of Carbon-Fibre Reinforced Skin-Stringer Panels', *In 'Composite Structures: Theory and Practice'*, ASTM STP 1383, Seattle, 1999.